LEVEL II

...randum Report 4633

# Spherical Acoustic Broadband Receiver

W. JAMES TROTT

*Acoustics Division*



December 16, 1981

12 42

251950

NAVAL RESEARCH LABORATORY
Washington, D.C.

SECURITY CLASSIFICATION OF THIS PAGE (When Data Entered)

| REPORT DOCUMENTATION PAGE | READ INSTRUCTIONS BEFORE COMPLETING FORM |
|---|---|
| 1. REPORT NUMBER: NRL Memorandum Report 4633 | 2. GOVT ACCESSION NO.: AD-A109273 |
| 3. RECIPIENT'S CATALOG NUMBER | |
| 4. TITLE (and Subtitle): SPHERICAL ACOUSTIC BROADBAND RECEIVER | 5. TYPE OF REPORT & PERIOD COVERED: Final report — FY-78 |
| 6. PERFORMING ORG. REPORT NUMBER | |
| 7. AUTHOR(s): W. James Trott | 8. CONTRACT OR GRANT NUMBER(s) |
| 9. PERFORMING ORGANIZATION NAME AND ADDRESS: Naval Research Laboratory, Washington, DC 20375 | 10. PROGRAM ELEMENT, PROJECT, TASK AREA & WORK UNIT NUMBERS: 65156-6010 |
| 11. CONTROLLING OFFICE NAME AND ADDRESS | 12. REPORT DATE: December 16, 1981 |
| | 13. NUMBER OF PAGES: 41 |
| 14. MONITORING AGENCY NAME & ADDRESS (if different from Controlling Office) | 15. SECURITY CLASS. (of this report): UNCLASSIFIED |
| | 15a. DECLASSIFICATION/DOWNGRADING SCHEDULE |

16. DISTRIBUTION STATEMENT (of this Report)

Approved for public release; distribution unlimited.



17. DISTRIBUTION STATEMENT (of the abstract entered in Block 20, if different from Report)

18. SUPPLEMENTARY NOTES

19. KEY WORDS (Continue on reverse side if necessary and identify by block number)

Electroacoustic transducer
Underwater sound transducer
Hydrophone array
Constant beamwidth transducer
Broad-frequency-band transducer
Surveillance tracking hydrophone

20. ABSTRACT (Continue on reverse side if necessary and identify by block number)

The development of a hydrophone array for determining signal bearing in three dimensions is described in theory and experiment. The array of omnidirectional elements, on a spherical surface is shaded in amplitude to produce a frequency-independent directional response. Design of omnidirectional elements is discussed.

DD FORM 1 JAN 73 1473 EDITION OF 1 NOV 65 IS OBSOLETE
S/N 0102-014-6601

SECURITY CLASSIFICATION OF THIS PAGE (When Data Entered)

CONTENTS



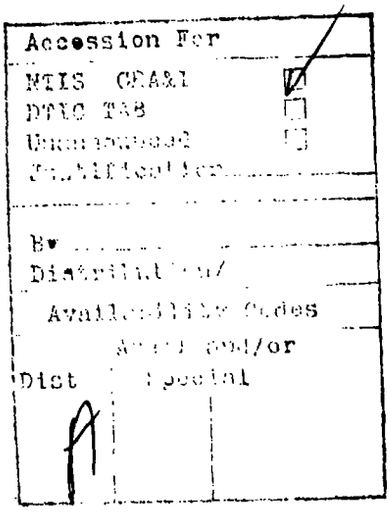

# SPHERICAL ACOUSTIC BROADBAND RECEIVER

## 1.0 INTRODUCTION

This report discusses, in theory and experiment, the development of a hydrophone array that is capable of determining the bearing of a received signal in three dimensions within a frequency range of two or more decades. A familiar approach, in two dimensions, is to use two coincident dipoles with axes in the x and y directions. The dipoles have directional responses of cos $\phi$ on the x-axis and sin $\phi$ on the y-axis, and the received signals can be designated $V_c$ and $V_s$. Azimuthal bearing is obtained from the ratio of the received signals from these two beams

$$\phi = \tan^{-1}(V_s/V_c) \tag{1}$$

The signals from the two dipoles can be combined in a resolver circuit to produce a steered beam in the bearing direction $\alpha$

$$V_c\cos\alpha + V_s\sin\alpha = V\cos(\phi - \alpha) = V_\alpha \tag{2}$$

Each beam is circularly symmetric about the beam axis. If a third coincident dipole has its axis in the z direction then the vertical angle

$$= \tan^{-1}(V_\alpha/V_z) \tag{3}$$

Thus the bearing of the received signal is determined. The simultaneous detection of another signal requires a parallel resolver and processing circuit. The 180° ambiguity in bearing is resolved by summing in quadrature the cosine pattern and a monopole to produce a $(1 \pm \cos\phi)$ pattern.

We start with an array of omnidirectional receiving elements uniformly distributed on a spherical surface. Signals from all elements are combined to produce the three orthogonal cosine-like beam patterns in the lower frequency range. Above the frequency at which the acoustic centers of the hemispherical sections are a half wavelength apart the hemispherical sections are directional and serve, by themselves, as a constant beam former over the upper frequency range. The theory for design of elements having omnidirectionality to a high frequency and the theory for element shading to produce a constant array directivity

Manuscript submitted August 13, 1981.

are developed. An array consisting of 416 elements was built and measurements made at the Underwater sound Reference Laboratory Detachment of Naval Research Laboratory. It is proposed that a fiber optic hydrophone could be designed on this concept for a three dimensional intercept receiver.

## 2.0 ELEMENT DESIGN

Capped piezoceramic cylindrical tubes are common elements in hydrophones and arrays. Langevin (1) calculated the electro-acoustical sensitivity of these elements for several end conditions (capped, shielded and exposed) and a variety of poling conditions (radial, longitudinal and tangential). His calculations were restricted to the omnidirectional frequency range. Langevin did not account for the effect of diffraction upon the electroacoustic sensitivity which begins to modify the sensitivity and directivity in the range of ka between 0.1 and 0.2, where k is the wave number in water and a is the radius of the outer cylindrical surface of the tubular element. The diffraction constant D of a hydrophone is defined as the ratio of the average sound pressure on a blocked diaphragm to the free-field sound pressure. The diaphragm is understood to be the sensitive area of the hydrophone, in this case the surface of the active element.

Trott (2) derived the diffraction constant for a finite length cylindrical surface with rigid end caps. This represents a piezoceramic tube, of any polarization, with shielded ends. The diffraction constants were also derived for a piston in the end of a finite length cylindrical baffle of the same radius as the piston. The constituent parts of a piezoceramic tube with capped ends are the cylindrical surface with rigid end caps, having one sensitivity level, plus a piston at each end of a rigid cylindrical baffle having another sensitivity level. The two sensitivity levels depend upon the material and the poling of the piezoceramic in addition to its dimensions. The relative contribution of each part is determined by the stress equations. If we break up Langevin's equations 10, 11 and 12 of reference 1, which express the voltage per unit of external sound pressure for radial (through the thickness of the tube) polarization, we have:

$$\text{(a)}\quad V/p_o = [g_p(1-r)/(1+r)] + g_t \text{ for shielded ends;} \tag{4}$$

$$\text{(b)}\quad V/p_o = a\{[g_p(1-r)/(1+r)] + g_t + g_t(1-r)\} \text{ for exposed ends} \tag{5}$$

where the first two terms are for the cylindrical surface and the third term is for the exposed end;

(c) $V/p_o = a[g_p(1-r)/(1+r) + g_t + g_t/(1+r)]$ for capped ends (6)

where the first two terms again are for the cylindrical surface and the third term is for the capped ends;

and where

$V$ = open-circuit receiving voltage
$p_o$ = external sound pressure (free-field sound pressure at low frequency ($N/m^2$)
$a$ = outer radius of the cylinder (m)
$r$ = ratio of the inner to outer cylindrical radius
$g_p$, $g_t$ = piezoelectric constants parallel and transverse to the polarization (Vm/N)

These equations are valid for $ka < 0.1$. We can express $p_o$ in terms of the free-field sound pressure $p_{ff}$ and the diffraction constant D

$$D = p_o/p_{ff} \tag{7}$$

Thus the free-field voltage sensitivity $M_h$

$$M_h = 20 \log_{10} (V/p_{ff}) = 20 \log_{10} D(V/p_o) \tag{8}$$

and equations (4), (5), and (6) become

$$V/p_{ff} = D_c a[g_p(1-r)/(1+r)] + g_t \tag{9}$$

for shielded ends, radially poled;

$$V/p_{ff} = D_c a\{[g_p(1-r)/(1+r)] + g_t\} + D_e a g_t(1-r) \tag{10}$$

for exposed ends, radially poled;

$$V/p_{ff} = D_c a\{[g_p(1-r)/(1+r)] + g_t\} + D_e a g_t/(1+r) \tag{11}$$

for capped ends, radially poled;

and where

$D_c$ = diffraction constant for the cylindrical surface, ends blocked

$D_e$ = diffraction constant for the ends active and the cylindrical surface blocked.

Similar equations are readily written for longitudinally and circumferentially (tangential) polarization.

Reference 2 gives the diffraction constants in magnitude and phase in graphic form. Reference 2 also shows graphically that the diffraction constant begins to affect the free-field voltage sensitivity between ka values of 0.1 and 0.2, and at higher values of ka the diffraction constant is a function of orientation, i.e., the element is no longer omnidirectional. Rogers and Zalesak (3) derived coefficients for the piezoceramic tube with the ends exposed (free-flooded ring) for $0.01 < ka < 5$ for the reciprocal transmitting current response. Such elements become directional at ka well below 0.1.

The A-42 probe hydrophone that was developed by NRL USRD has a radially poled, capped piezoceramic tube. The dimensions are 3.2 mm in diameter, 3.2 mm in length, and 0.79 mm in wall thickness with magnesium caps 0.79 mm thick. This element is omnidirectional up to 35 kHz. Above this frequency, the axial sensitivity diminishes relative to the radial direction and drops to a minimum at around 100 kHz. Above 100 kHz, the pattern develops 4 lobes. This pattern shape is primarily due to the radiation from the two end caps. Equation 11 shows that piezoceramic tube wall thickness does affect the relative contribution from the end caps. Some theoretical calculations show that the maximum variation from omnidirectionality for the A-42 in the region of 100 kHz is 10 dB. If the wall thickness was reduced from 0.79 to 0.4 mm the variation from omnidirectionality would be 4 dB.

The study that produced Ref. 2 was primarily a study of element design for this project. In trying to obtain a maximum size element that would be omnidirectional up to 200 kHz a computer program, SHIP (Ref. 4), was used that shows the far-field sound radiation from cylindrical sources for various velocity distributions. These included: (1) a unit velocity on the outside surface, (2) a unit velocity on the ends. In each case all other surfaces had zero velocity. By combining these velocities in the proper ratios the radiation characteristics of piezoceramic tubes poled in thickness, height or circumference with the ends shielded or capped are calculated. Radiation from the ends reduced the omnidirectional frequency range with directionality becoming a maximum when the distance between the acoustic centers of these two pistons is a half wavelength. For a height to diameter ratio of 1 this effect was maximum at $ka = 1.1$, and for a height to diameter ratio of 1.5 it was a maximum at $ka = 0.75$. These end caps effect the directivity from $ka = 0.2$. The computations showed that the maximum omnidirectional frequency range is obtained from piezoceramic tubes having the ends shielded and a height to diameter ratio of 1.5. Table 1 shows the maximum variation from omnidirectionality as a function of ka for height to diameter ratios of 1, 1.5 and 2.

TABLE 1

VARIATION FROM OMNIDIRECTIONALITY

FOR

PIEZOCERAMIC TUBES HAVING SHIELDED ENDS

| | RATIO HEIGHT/DIAMETER | | |
|---|---|---|---|
| ka | 1 | 1.5 | 2.0 |
| 0.116 | 0.04dB | 0.02dB | 0.01dB |
| 0.231 | 0.15 | 0.08 | 0.03 |
| 0.347 | 0.35 | 0.20 | 0.05 |
| 0.462 | 0.64 | 0.39 | 0.06 |
| 0.578 | 1.05 | 0.66 | 0.06 |
| 0.693 | 1.59 | 1.01 | 0.16 |
| 0.809 | 2.28 | 1.39 | 0.49 |
| 0.924 | 3.09 | 1.69 | 1.23 |
| 1.040 | 4.01 | 1.77 | 2.56 |
| 1.155 | 4.93 | 1.46 | 4.63 |
| 1.271 | 5.69 | 0.64 | 7.61 |
| 1.386 | 6.03 | 0.70 | 12.06 |
| 1.502 | 5.76 | 2.47 | 20.80 |
| 1.617 | 5.03 | 4.66 | 31.7 |
| 1.733 | 4.33 | 7.35 | 24.7 |
| 1.848 | 3.69 | 10.92 | 23.66 |

We therefore chose to design an element in the form of a piezoceramic tube with shielded ends and a height-to-diameter ratio of 1.5. Even when this element becomes directional, the axial sensitivity is above that in the radial direction and should be preferable for this spherical array configuration, where the elements are mounted with the ceramic tube cylindrical axis in the radial direction of the spherical surface. Figure 1 shows the measured sensitivity of the A-42 probe in relation to the theoretical axial and radial sensitivity of an element having the same diameter, a height to diameter ratio of 1.5, and the ends shielded. The next problem was how to build an element with shielded ends without exposing pressure release material to the sound field. One way that has been used is to mount the piezoceramic tube on a spool shaped insulator with layers of onion skin paper as the pressure release material between the spool and the inside surface, and paper washers between the ends and the spool rims. If the exposed edge of the washers is in a very thin gap, then a rubber coat over the element will have enough shear stiffness to shield the pressure release material from the sound field. Some element experiments were performed using ceramic elements from laboratory stock.

## 2.1 ELEMENT EXPERIMENTS

A radially poled ceramic tube at low frequencies expands in circumference and length, in phase, as the thickness is reduced. If a plastic ring is cemented to each end of the ceramic tube so that it expands with the element circumferential expansion but its axial length shortens in relation to its Poisson ratio, this will reduce the total length expansion of the ceramic plus-plastic rings. A piezoceramic element 3/4 in. X 3/4 in. X 1/8 in. of ceramic B, was used for the experiment. Lucite rings of cross section 1/8 in. x 5/32 in. were epoxied on the ends of the ceramic B. A 7/16 in. aluminum mandrel was fitted loosely inside with a 1/32 in. layer of Corprene between the mandrel and the ceramic B. This unit showed, by calibration, to be omnidirectional within 1 dB up to 25 kHz, equivalent to 150 kHz if scaled down to the dimensions of the A-42 element, as in Fig. 1.

From Ref. 5, for an element that is again radially poled, the velocity of an end, $u_2$, is

$$u_2 = (h_1/2b)u_b \qquad (12)$$

where

$h_1$ = the axial tube length or height

b = the mean tube radius

$u_b$ = the mean radial velocity.

The outside cylindrical surface velocity is in phase with $u_2$

$$u_3 = (1 + t\, d_{33}/2b\, d_{31})\, u_b \tag{13}$$

where

t = the tube thickness

$d_{33}$, $d_{31}$ = the strain constants, strain/field (m/V).

For a height poled ring

$$u_2 = (h_2 d_{33}/2b d_{31})u_b \tag{14}$$

$$u_3 = (1 + t/2b)\, u_b \tag{15}$$

out of phase with $u_2$.

If we pole, in height, a ring section on each end of a radial poled center section and if

$$\underset{\text{(height poled)}}{(2u_2)} = \underset{\text{(radial poled)}}{-(u_2)} \tag{16}$$

then the desired zero end displacement or velocity can be achieved up to the frequency just before radial resonance when the resonance mode reverses the phase of the end velocity in relation to the radial velocity. For the radially poled element the radial velocity at the mean radius is

$$u_b = j\,\omega\, d_{31} V(b/t) \tag{17}$$

with

$\omega$ = the angular frequency

V = the driving voltage

and

$$u_2 = (h_1/2b)(b/t) j\, d_{31} V = (h_1/2t)(j\, d_{31} V \quad (18)$$

(radial poled)

For the height poled end rings

$$2u_2 = (h_2/b)(d_{33}/d_{31})(j\, d_{31} V)(b/h_2) \quad (18a)$$

(height poled)

$$= j\, d_{33} V \quad (18b)$$

For zero end velocity of the composite tube element length,

$$-h_1 = 2\, t(d_{33}/d_{31}) \quad (19)$$

if all sections are electrically in parallel.

We want an overall height to diam = 1.5 for omnidirectionality over a maximum frequency range with zero end velocity. Capping to decouple the inner radial velocity from the sound field will reduce 1 the radial velocity, $u_3$, in the region of the tube ends due to the stiffness of the end cap. By connecting the two end sections in series, and then in parallel with the center section, the factor 2 is eliminated in Eq. (19) and

$$h_1 = t(d_{33}/d_{31}).$$

with $d_{33}/d_{31} = -0.461$ for ceramic material Navy II (Channel 5500)

and making the radial velocity of the center and end sections equal and the height-to-diameter equal to 1.5, the relationship between a and t is derived to be

$$6a^2 - 15.86\, at + 6.89\, t^2 = 0 \quad (20)$$

For the element used

$a$ = 0.25 in. outside radius

$b$ = 0.119 in. thickness

$h_1$ = 0.259 in. (radial poled height)

$h_2$ = 0.245 in. (height poled height)

There were no cemented joints in this element. The 1/2 X 3/4 in. elements were electroded in the center and at the ends and polarized

in three steps. A laser interferometer was used to measure the radial and axial displacement when these elements were capped and driven in air with 10 V. The end caps did affect the radial velocity but the end velocity was substantially reduced. Further adjustment could be accomplished by removing some of the electrodes or adding series capacitance to one of the poled sections to obtain the equality of equation 19. Calibration is required to establish equality. For a radial poled element with capped ends, the sensitivity in the radial direction is above the sensitivity in the axial direction, i.e., above ka = 0.2. For a height poled element the relationship is the reverse. A calibration will show which section is dominant, requiring a series capacitance to reduce its dominance to yield the omnidirectionality over the maximum frequency range. A hydrophone was constructed for test by NRL USRD.

Simultaneously with this experimental effort, material was purchased for producing the element using the more conventional method that was mentioned in introducing this section, Fig. 2. Height poled piezoceramic rings were used to insure that, if the end caps did move, the directivity would be predominantly axial and not radial as would occur if the elements were poled radially or through the thickness of the tube. The steatite spool was in two parts to make assembly of the element easy. This conservative design was used.

The cabling for an array of this type must be acoustically stiff and small, with respect to the wave length, or the large amount of cabling for the 416 elements would produce transmission loss through the spherical array. Coaxial cable is used that consists of a 0.034 in. copper tube, 0.0035 in. thick, with an 0.008 in. silver plated, copper-clad steel center conductor. The acoustic compliance of this coax must be less than the compliance of the volume of water it displaces and is given by

$$C_a = (\text{Volume})\ a/2Et(5 - 4\sigma)\ \ (\text{Volume})/\rho_o c_o^2 \qquad (21)$$

Where $C_a$ is the acoustic compliance of a unit length of the coax equated to the acoustic compliance of the equal volume of water,

$a$ is the outside radius of the coax,
$t$ is the coax wall thickness,
$E$ is the Young's modulus of the cooper tube,
$\sigma$ is the Poisson ratio of the copper tube,
$\rho_o$ is the density of the displaced water,
$c_o$ is the speed of sound in the water.

Using the cable characteristics shows that the condition of Eq. (21) is met.

That is, $5.4 \times 10^{-12} < 4.4 \times 10^{-10}$ .

The element must be coated with a compliant material that is impermeable to water. Normally one would use neoprene or butyl rubber for this purpose but it was desired to have a material that could be deaerated in a vacuum chamber so the elements could be dip coated under vacuum. A liquid polysulfide was obtained from the Thiokol Chemical Corporation and mixed with Thermoset 316 Epoxy. After several trials it was found that a good cure and compliant coating was obtained from a mixture comprising 9 g of 316 Resin, 3 g of hardener, and 6 g of LP-3 polysulfide. NRL USRD measured the permeability of a disc of this material. The average water permeability was 620 compared with permeabilities of neoprene of 440 and natural rubber of 529. The material was considered to be suitable for the purpose. The elements were cured overnight at 140°F. A second coat was applied by dipping without vacuum. The combination of liquid polysulfide and epoxy converts to a flexible, resilient rubber with the strength, adhesive and electrical properties of epoxy resins and is suitable for dip coating piezoceramic elements.

Sample elements were calibrated at NRL USRD in June, July, August and September of 1977. In the September calibration some of the elements proved to be omnidirectional to within 1 or 2 dB up to 100 kHz except for a direction of sound incident along the coax cable. The elements were not alike in sensitivity as a function of frequency. More development was required. However, because of earlier project delays it was desirable to establish feasibility within the fiscal year and it was concluded that the predominantly axial radiation was sufficient to yield the desired cosine type beam pattern.

## 3.0 ARRAY DESIGN

Trott (6) prepared design parameters for elements on a spherical surface shaded to produce a constant directivity. Since the array is to operate over two or more decades, the spherical surface must be acoustically transparent. No rigid baffle would be rigid (non resonant) over such a wide frequency range with ka values from 0.1 to 36 where a, in this case, is the radius of the sphere and k the wave number. Rogers and Van Buren (7) derived the theory for this constant beam transducer array on a rigid baffle. Jarzinsky and Trott (8) showed that the theory also applied to an array on an acoustically transparent spherical surface. Cosine shading of a spherical surface is the equivalent of a sphere vibrating sinusoidally, as a unit, along the beam axis. The free-field voltage sensitivity of such a transducer is shown in reference 6. The sensitivity increases linearly with frequency up to a peak at $ka = \sqrt{2}$ and then decreases inversely with frequency. For an acoustically transparent spherical surface, containing omnidirectional elements shaded in proportion to the cosine of the angle from the beam axis, the

free-field voltage sensitivity increases 6 dB per octave to a maximum at ka = 2.082 and then decreases 6 dB per octave with successive nulls at ka = 4.49, 7.725, 10.9, etc. The receiving sensitivity is proportional to the spherical Bessel function of order 1 and the radius a of the sphere (Ref. 8). Figure 3 shows the relative free-field voltage sensitivity for the full spherical array, i.e., the two hemispheres shaded in magnitude proportional to the cosine and connected in series, balanced output to obtain sign a reversal between halves. To avoid the low cusp Fig. 3, we can receive on one hemispherical array with an unbalanced output, for ka >3 . Beam patterns for this condition, a hemispherical array, were calculated and described by Rogers and VanBuren (7). Patterns were shown for a constant beam axis sensitivity. Maximum and minimum levels were shown in the transmitting current response (absolute level of patterns) but not taken into account in describing the patterns. This is standard procedure for calibration data presentation but it showed beam differences between the angles of 20 and 90 degrees that exaggerated the true condition. In shading a hemisphere in proportion to the cosine of the angle, the shading cuts off at zero (axis crossing at 90°) but the derivative of the shading function is unity (sin 90°). This cut-off produces maxima and minima in the axis sensitivity as a function of frequency and the transmitting current response as was shown in Fig. 3 of Ref. 7. Due to shading symmetry the variation in level of sensitivity and response is greatest on the beam axis (0°). If the patterns had been plotted to an absolute level as transmitting beam patterns, the skirts of the beam patterns would nearly have coincided. Two patterns, cosine and sine shaded, from this theory were used to calculate the error in bearing measure that is caused by these maxima and minima. The curves of Eq. (1),

$$\phi = \tan^{-1}(V_s/V_c), \text{ are shown in Fig. 5.}$$

Jarzinski and Trott (8) derived a shading function for which the value and the first derivative of the function are zero at this cut off. The shading function is

$$f(\phi)=(n/(4n+2))\cos^{n}\phi+ 1/2\cos^{(n+1)}\phi+((n+1)/(4n +2))\cos^{(n+2)}\phi. \qquad (22)$$

The lowest order and broadest beam occurs for n = 1 and

$$f(\phi)= (1/6)\cos \phi + 1/2\cos^{2}\phi/ + (1/3) \cos^{3}\phi. \qquad (23)$$

This is predominantly a cosine-squared beam but the beam is far more constant, there are no maxima and minima in the axial response that occur for cosine shading over the hemisphere. The bearing measure is shown in Fig. 6. Figure 7 shows the bearing measure in a way that shows the cosine-squared nature of the beam. Taking the square root of the signal, prior to the ratio, increases the sine-pattern-signal in the region of 0° and only adds to the bearing measure

error. Additional signal processing is required to rotate the azimuth beam for determining the vertical angle bearing.

With this shading, the two hemispheres, connected in series with balanced output, produce a good cosine pattern up to ka =3. Therefore, the target azimuth angle is obtained from the two beams as shown in the Eq. 1 and the vertical angle from Eq. 3.

Above ka = 3 we must use only hemispherical arrays to avoid the nulls (Fig. 3) which occur when the distance between the acoustic centers of the two hemispherical arrays is a multiple of a wavelength. For cosine shading the first null occurs at ka = 4.49. For the shading function of Eq. 23 the first null is at ka = 4.1. In the range of this null the beam is unsuitable for measurement of bearings. The far-field pattern of the hemispherical array is omnidirectional at low values of ka and approaches the cosine square directivity at ka=3.

To obtain the vertical bearing at azimuth angle $\alpha$, the azimuth beam must be steared in the direction of $\alpha$. For the vertical bearing the directed azimuth beam can be obtained by signal processing, for ka >3

$$V = \cos^2(\theta + \alpha) = V_c \cos^2\alpha + V_s \sin^2\alpha + 2(V_c V_s)^{1/2} \sin\alpha \cos\alpha \qquad (24)$$

$$\text{and } \theta = \tan^{-1}(V_\alpha / V_z) \qquad (25)$$

This beam pattern should be the same in the vertical plane as in the azimuth plane around the beam axis ($\theta = 90^\circ$) and more like the shading function in the region of $\theta = 180^\circ$ and $0^\circ$. Bearing measure versus vertical angle $\theta$ is shown in Fig. 8.

Thus three dimensional target tracking is possible with three orthogonal beams formed by proper shading and signal processing from omnidirectional elements distributed over an acoustically transparent spherical surface. Below ka = 3 the full spherical array is used by connecting the hemispherical arrays in series, balanced output, to produce the cosine pattern. To determine the directional ambiguity ($\phi$ or $\phi + 180^\circ$) a single element at the center of the spherical surface is added in quadrature to produce a $(1 + \cos\phi)$ pattern. Above ka = 3 we use one hemisphere to produce the approximately $\cos^2\phi$ pattern. The locus of the acoustic center of the hemispherical array is shown in Fig. 9, as a function of ka, in terms of the fraction of the sphere radius a from the center of the spheres. Thus the $180^\circ$ ambiguity above ka = 3 can be resolved by detecting the time delay of the back hemispherical array with respect to the front hemispherical array. This will vary from 0.03 msec at $45^\circ$, ka = 3 to 0.05 msec at higher values of ka.

Although a frequency correction would be required for the most accurate bearing determination as shown in Fig. 7, three dimensional target tracking can be achieved over 2 or more decades by this proposed technique. Array sensitivity varies by less than 20 dB over 2-1/2 decades if the peak sensitivity and switchover frequency from full spherical to hemispherical array occurs at about the geometric mean of the operating frequency extremes.

## 4.0 EXPERIMENTAL TRANSDUCER

The experimental transducer consists of 416 elements. A total of 500 elements were built and sorted out in order of their capacitance and dissipation. The cable capacitance was 58 pF. The element capacitances were calculated to be 55 pF. The element sensitivity was calculated to be -200 dB re 1V/ Pa. The shunt capacitance of the cable should yield an end-of-cable sensitivity of -206 dB re 1V/ Pa. The end-of-cable measured capacitance varied between 104 and 121 pF. Elements were used that were in the range of 108 to 121 pF with dissipation less than 0.02. The few measured elements showed sensitivities in the range of -210 dB re 1V/ Pa indicating some loss of sensitivity due to end cap movement and some variation of sensitivity with frequency. Calibration of all elements prior to assembly of the array was not possible. The elements were distributed evenly over two polycarbonate hemispherical shells, 0.040 inch thick, having a negligable loss in the sound field, only 0.6 dB at 200 kHz. The element distribution was in the form of rings at $\phi$ = 0°, 10°, 31°, 42°, 52°, 62°, 72°, 82.5° and 90°. The 36 elements per ring at 82.5° and 90° were arranged so that the distribution around the x, y and z axes would be similar. Element shading was corrected for the average elemental area in each ring position. Although the final assembly would require 3 operational amplifiers connected to each element for producing the three orthogonal beams, an initial test of one beam was done with the elements in each ring connected in parallel and a series capacitor used for shading. Each ring, with its series capacitor, was then connected in parallel with the other rings to yield two wire outputs from each hemispherical array. The two arrays were then connected in series, balanced output for calibration from 0.5 to 20 kHz and the individual arrays, with unbalanced output, were calibrated from 10 to 200 kHz. Figure 10 shows the element components and an assembled unit dip coated in epoxy polysulfide Fig. 11 shows one hemispherical array assembled and a second partially assembled. Special tools and fixtures were made to assemble elements into the shell; the rubber bands showing in Figure 10 held the elements in position until the epoxy, bonding them to the shell, had hardened. Figure 12 shows the terminal board and one ring array output with its shading capacitors. Figures 13 through 16 show the constant directivity for the spherical array in the frequency range of 0.5 to 10 kHz. Marked on the figures are the levels of a cosine direc-

tivity for a comparison. The free-field voltage sensitivity for balanced output of the spherical array is shown in Fig. 17. It approximates the 6 dB per octave predicted by theory.

Figures 18 and 19 show the constant directivity of each hemisphere in the frequency range 10 to 30 kHz. Above 30 kHz all data was extremely variable. On the side of the Fig. 18 is the azimuthal shading level which should approximate the directivity level.

Figure 20 shows the calculated directivity levels for the frequency range 5 to 100 kHz for comparison with Figs. 18 and 19. The measured free-field voltage sensitivities in the directions of 0° and 180° for each hemispherical array are shown in Figs. 21 and 22. The sensitivity should have peaked around 12 kHz and decreased 6 dB per octave above the maximum. Obviously the elements aren't sufficiently omnidirectional to produce the constant directivity and the concomitant 6 dB per octave roll off at frequencies above the maximum. The 0° and 180° sensitivities show as much as 10 dB of transmission loss through the shell and array of coax cables. Since the shell should only reduce the signal by a maximum of 0.6 dB at 200 kHz and the coax is 80 times as stiff, individually, as the displaced water volume, the loss must be due either to air in the epoxy joints or in the filling oil, or to scattering from the mass of cable. The experimental unit did not meet the objective of a broadband receiver for signals over the full frequency range of 0.5 to 200 kHz.

## 5.0 SUMMARY OF DATA

Although the array seemed to approach the desired goal of a constant directivity from 0.5 to 200 kHz, the experimental array showed a reasonable cosine pattern for the full array only to 8 kHz, not to the 17 kHz required (ka = 3). The hemispherical arrays showed a degree of constant directivity in the range of 10 to 30 kHz range but the elements were not sufficiently omnidirectional nor were the sensitivities sufficiently the same to produce the interference between ring arrays to yield a constant directivity and concomitant 6 dB per octave drop in free-field voltage sensitivity. In view of the difference in array sensitivity at 0° and 180° there must be trapped air producing a transmission loss. An alternate design is required to insure omnidirectionality of elements, an acoustically transparent sphere, and equality in element sensitivity. These appear to be the major problems with the experimental unit.

## 6.0 PROPOSED ALTERNATIVE DESIGN

Three conditions are considered to have caused the failure of the experimental transducer to meet the objectives. The elements were not sufficiently equal in sensitivity nor sufficiently omnidirectional to

produce constant directivity over the wide frequency range. Scattering from the large number of coax cables or air bubbles trapped in the epoxy bonds produced 10 dB or more transmission loss through the spherical array. An alternative design is proposed that should correct these problems with the first experimental unit.

A considerable effort has been initiated in the Navy using an optical glass fiber as a sound sensitive hydrophone element (Ref. 9). Two fibers are compared, optically, in an interferometer. One is immersed in the sound field and changes in the index of refraction and in length with the action of the sound pressure. The second is isolated from the sound field and acts as a reference optical length fiber. A coherent laser light is common to both fibers and its modulated light level is detected as an electrical voltage from the interferometer detector at the frequency of the acoustic signal, Ref. 9. If the optic fiber is wound in a coil to produce an omnidirectional receiver the sensitivity is constant with frequency as in a piezoelectric material. The fiber is small (core diameter 2.5 um) and uniform in sensitivity, strain per unit of sound pressure. The fiber can be wound on a spherical shell and the optical sensing package mounted exterior of the array to insure array transparency. It seems that the three causes for the first experimental failure are eliminated when the fiber optic hydrophone principle is used.

A fiber coil, like a free-flooded magnetostrictive or piezoceramic ring, has a predominantly toroidal directivity due to the change in length with pressure. J. Jarzinsky of NRL has measured the directivity of a close-packed coil and observed this toroidal pattern. He has also wound a coil on a thick polycarbonate cylindrical tube and varied the coil turn density along the tube in proportion to a Gaussian function. A shaded directivity was measured. This method of shading could be used in shading the density of fibers on a spherical surface for the constant beamwidth transducers. Three of these fiber windings could be nested with a common, spherical-surface center with the beam axes directed along the three coordinate axes.

Separate fibers would be used for each hemispherical surface. At low frequencies the fiber on one hemisphere would act as the reference to the fiber on the other hemisphere, a gradient hydrophone principle. At higher frequencies, above the maximum in Fig. 3, the reference fiber would be an auxiliary fiber isolated from the sound field. Thus a similar sensitivity level would exist for the fiber optic hydrophone; 6 dB per octave rise at low frequencies as a gradient hydrophone (full spherical array) and 6 dB per octave drop as a constant-beam, pressure-sensing hydrophone (hemispherical array) in the upper frequency range. The acoustic compliance of the fiber is less than 5% of the compliance of the displaced volume of water thus meeting one requirement of array

transparency. Secondly, the fiber size, 2.5 um, is much less than the sound wave length in water. A research program to determine the feasibility of using the fiber optic hydrophone as the three dimensional intercept receiver would consist of:

(1) determining, by existing computer programs, the distribution of the turn density of optical fiber on a spherical surface to yield the constant directivity, Eq. 22, using the change in index of refraction with pressure,

(2) machining a polycarbonate spherical shell with a fine groove for locating the optical fiber in accordance with the shading function,

(3) assembling and testing the fiber optic hydrophone for sensitivity and directivity. (The sensitivity as a function of frequency should match the curve of a piezoelectric array. In principle, measurements would consist of using both hemispheres at low frequencies as comparison fibers in the interferometer, and a single hemisphere with a reference fiber, acoustically shielded, at higher frequencies.)

(4) winding the second and third orthogonal array fibers over the first for the complete broadband receiver.

## 7.0 SUMMARY

Theory predicts that a broadband constant directivity transducer can be built by shading an array of elements on a spherical surface. The spherical surface can be rigid (Ref. 7) or acoustically transparent (Ref. 8). For an acoustically transparent spherical surface, the elements must be omnidirectional so that the interference between all the elements can yield the constant directivity and the -6 dB per octave change in the free-field voltage sensitivity. The design of elements to achieve the required broadband omnidirectionality was theoretically developed (Ref. 2) and experimentally verified.

A technique for using such an array to receive signals and to determine signal bearing in three dimensions was developed using the constant beam theory (Ref. 8). An experimental array was constructed and calibrated over the range of 0.5 to 200 kHz to determine beam patterns and free-field voltage sensitivity. Only limited success was achieved due to element design and array construction problems. A new design is proposed to avoid the problems of lack of element constant sensitivity with frequency, broad-band element omnidirectionality, and array acoustic transparency that caused the experimental transducer to fail to meet the specified objectives.

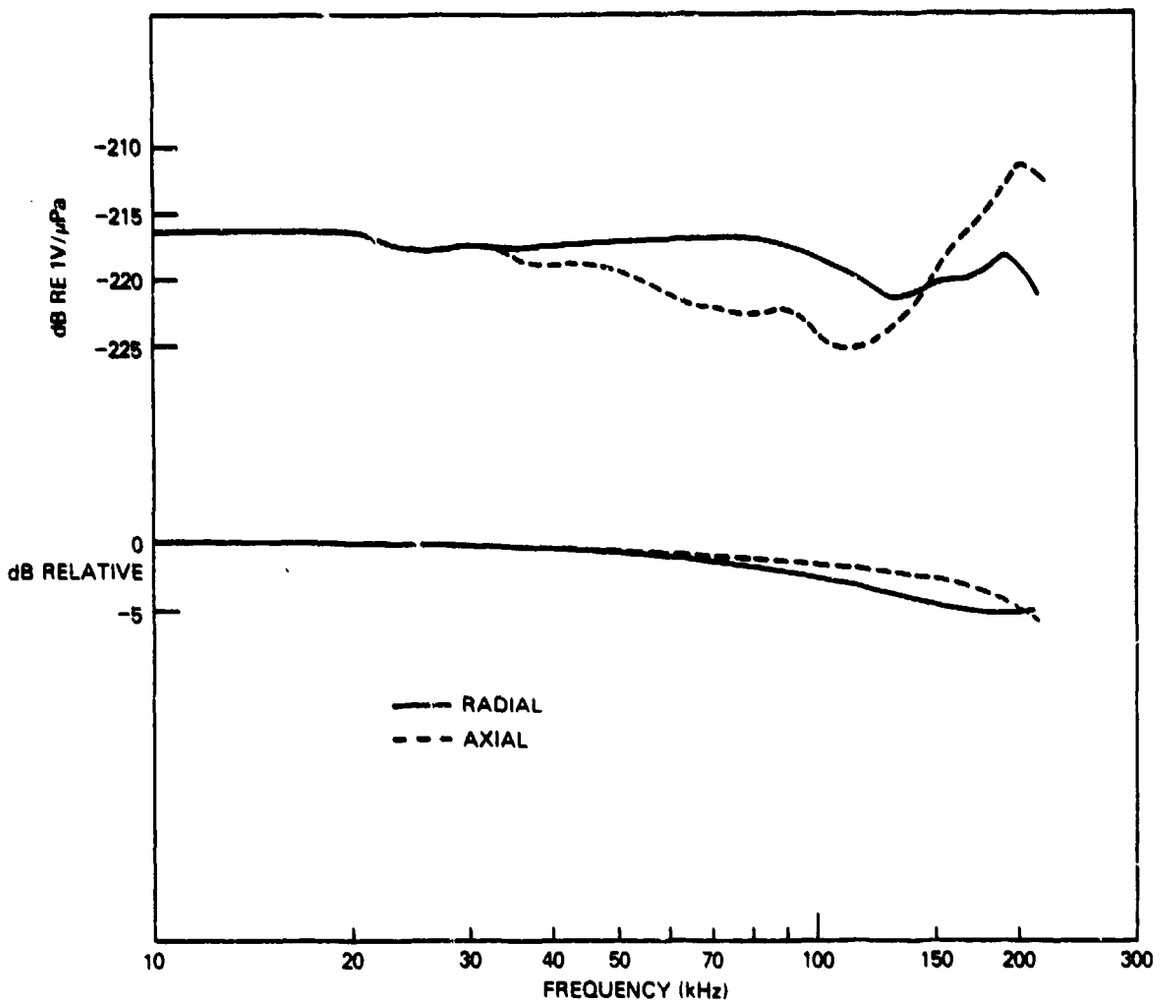


Fig. 1 — Free field voltage sensitivity. A-42 top pair of curves.

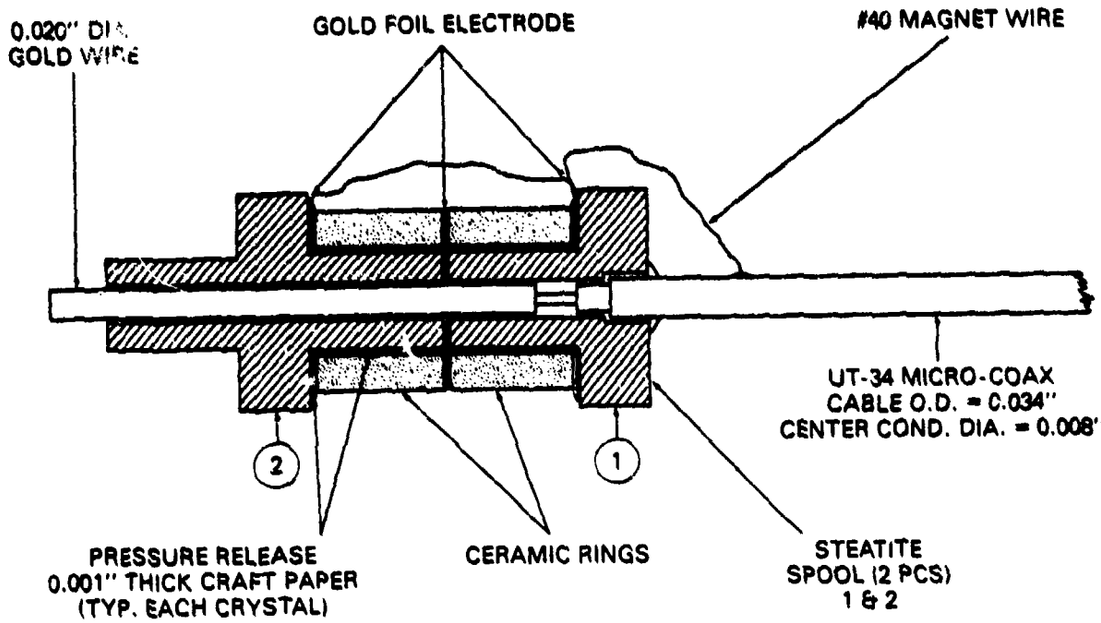


Fig. 2 — Experimental array element

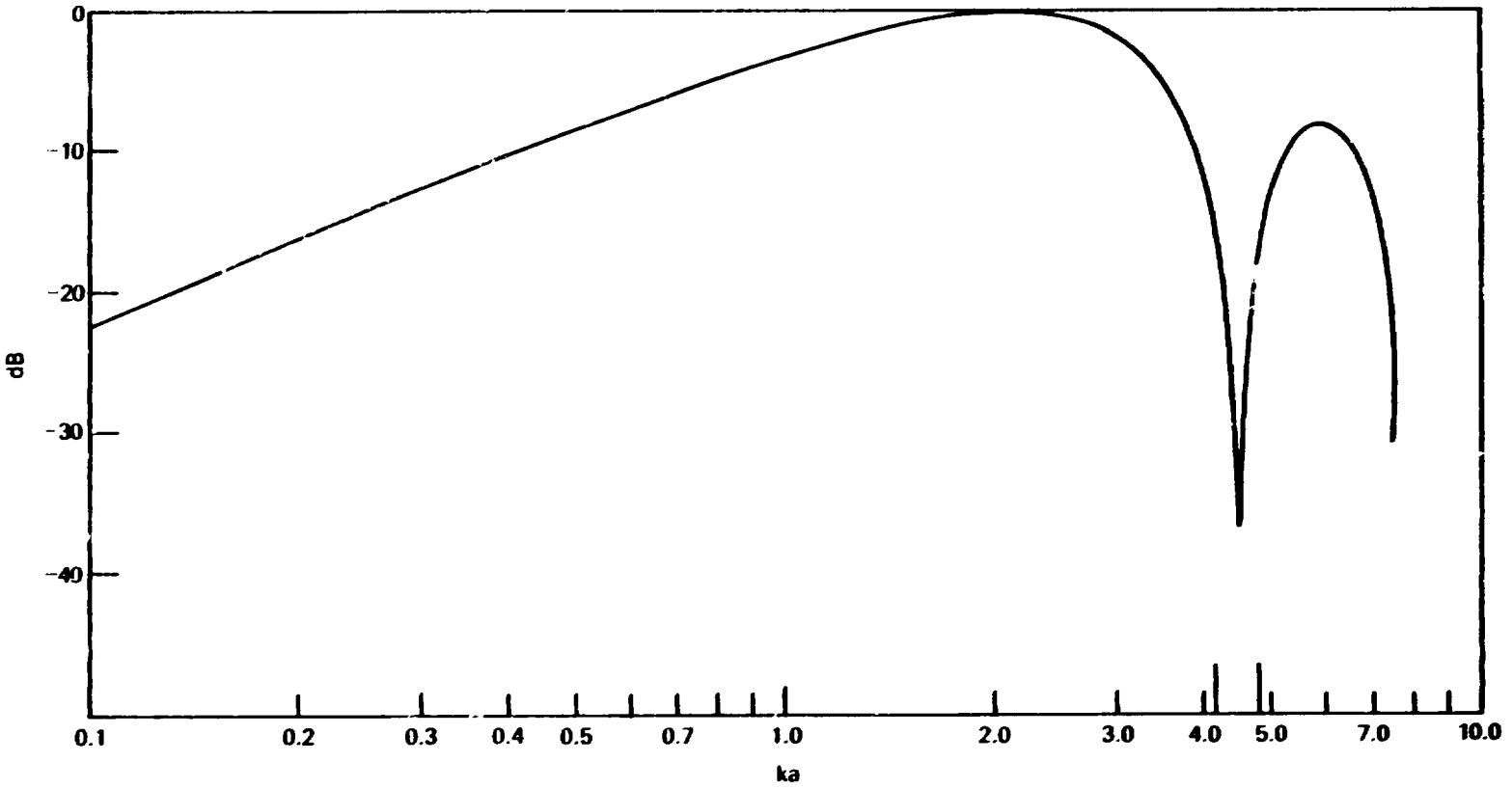


**Fig. 3 — Relative sensitivity level for a cosine shaded spherical array on a rigid baffle**

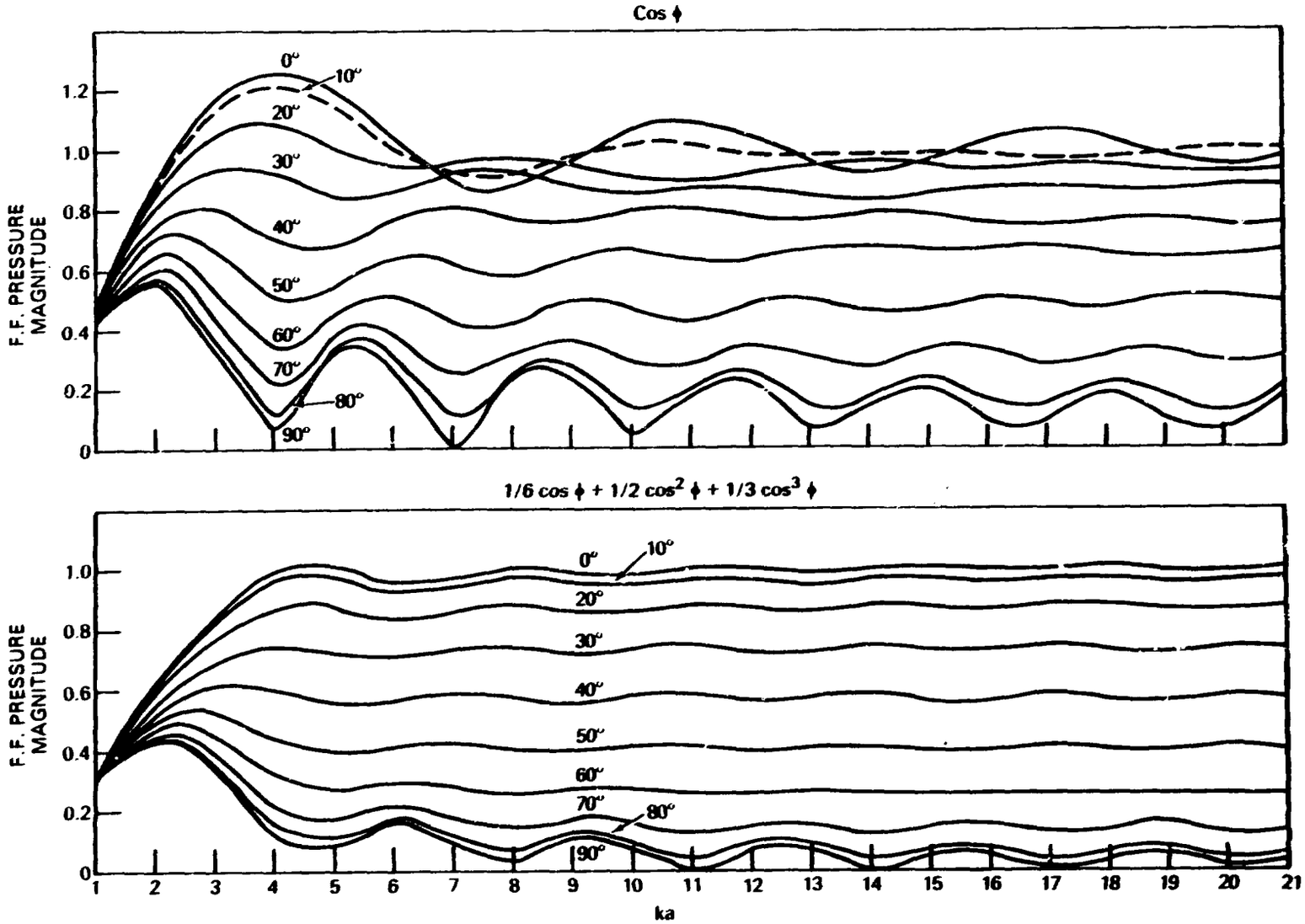


Fig. 4 — Hemispherical shading

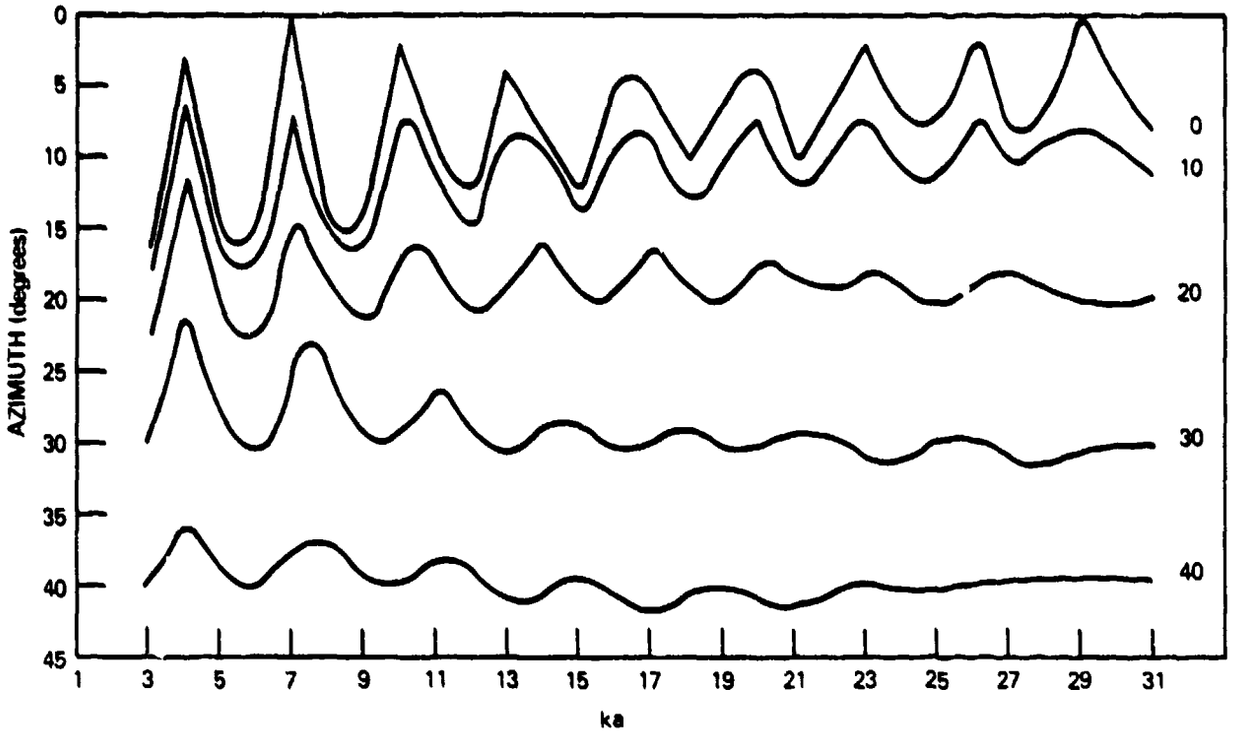


**Fig. 5 — Bearing measure for cosine shading over a hemisphere**

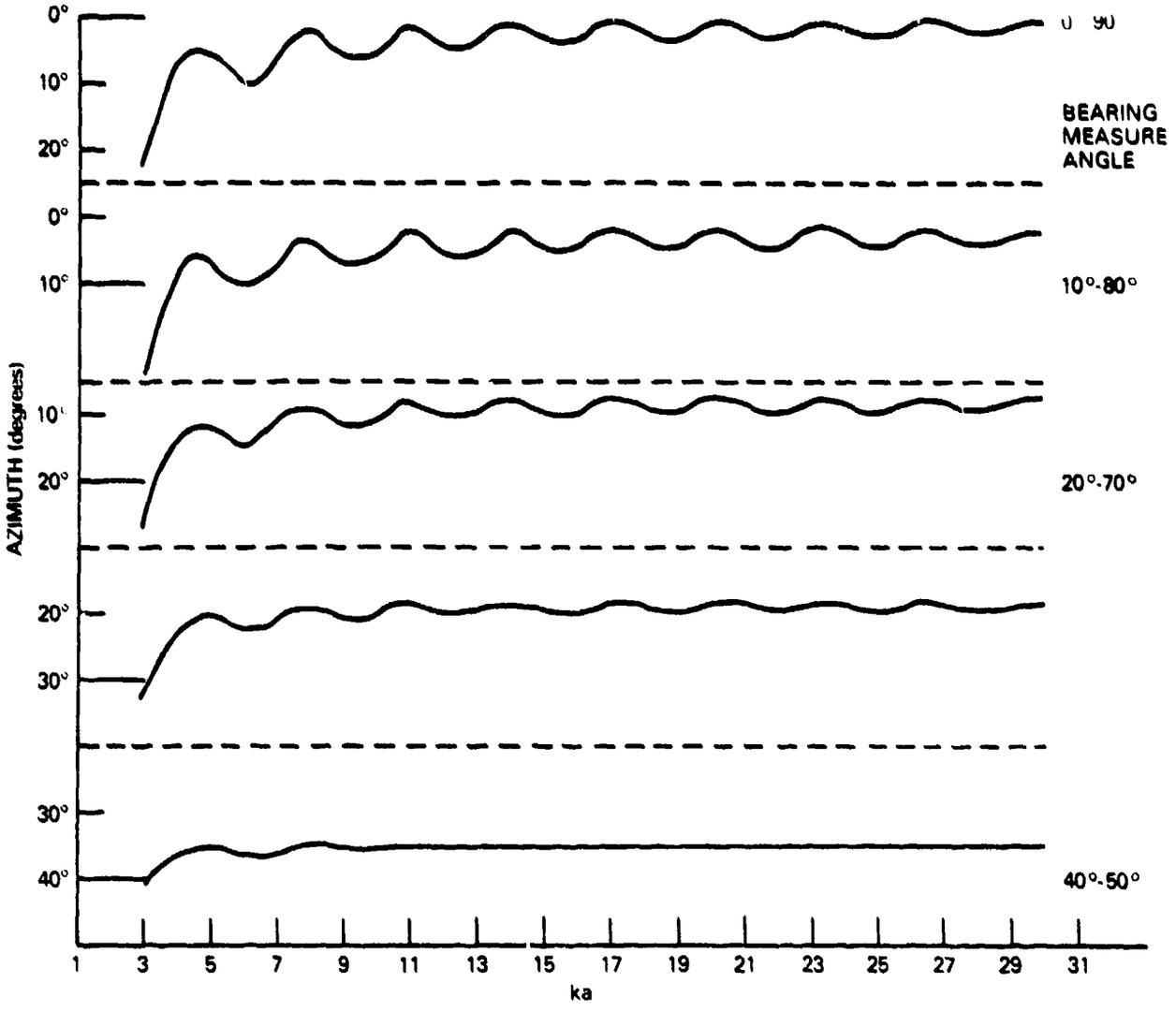


Fig. 6 — Bearing measure for shading over a hemisphere

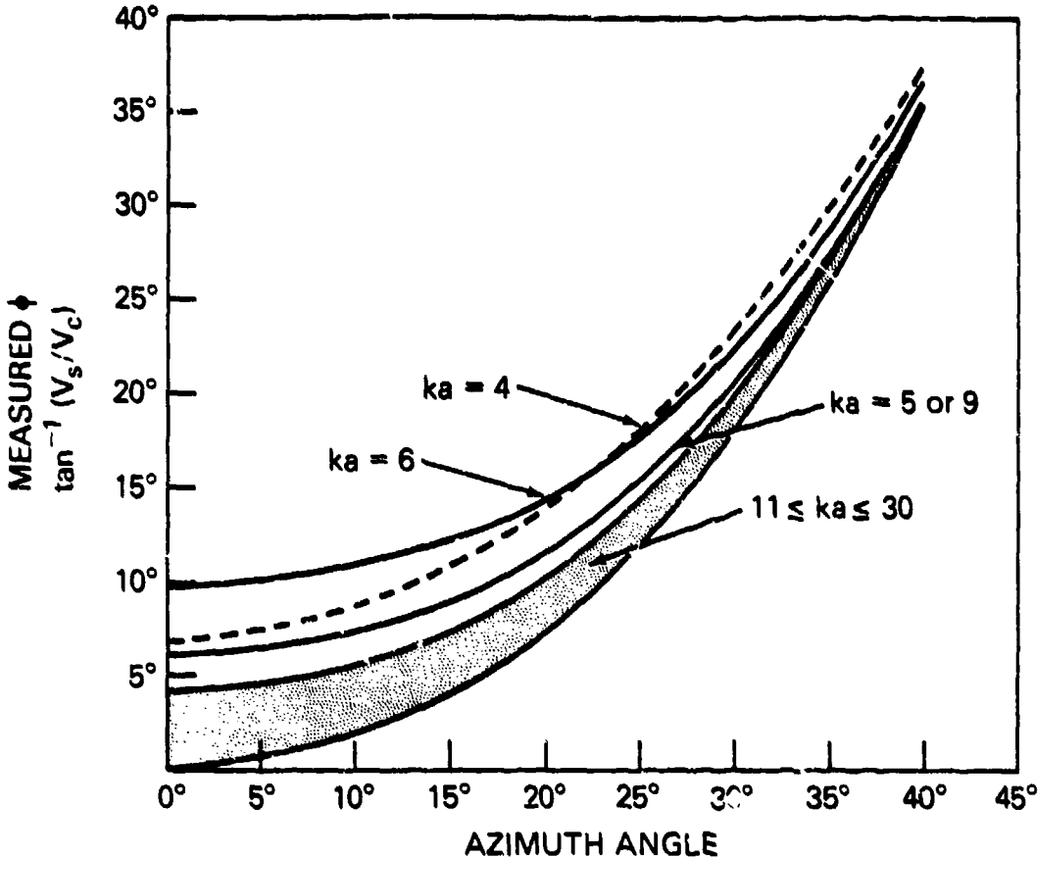


**Fig. 7 — Bearing measure**

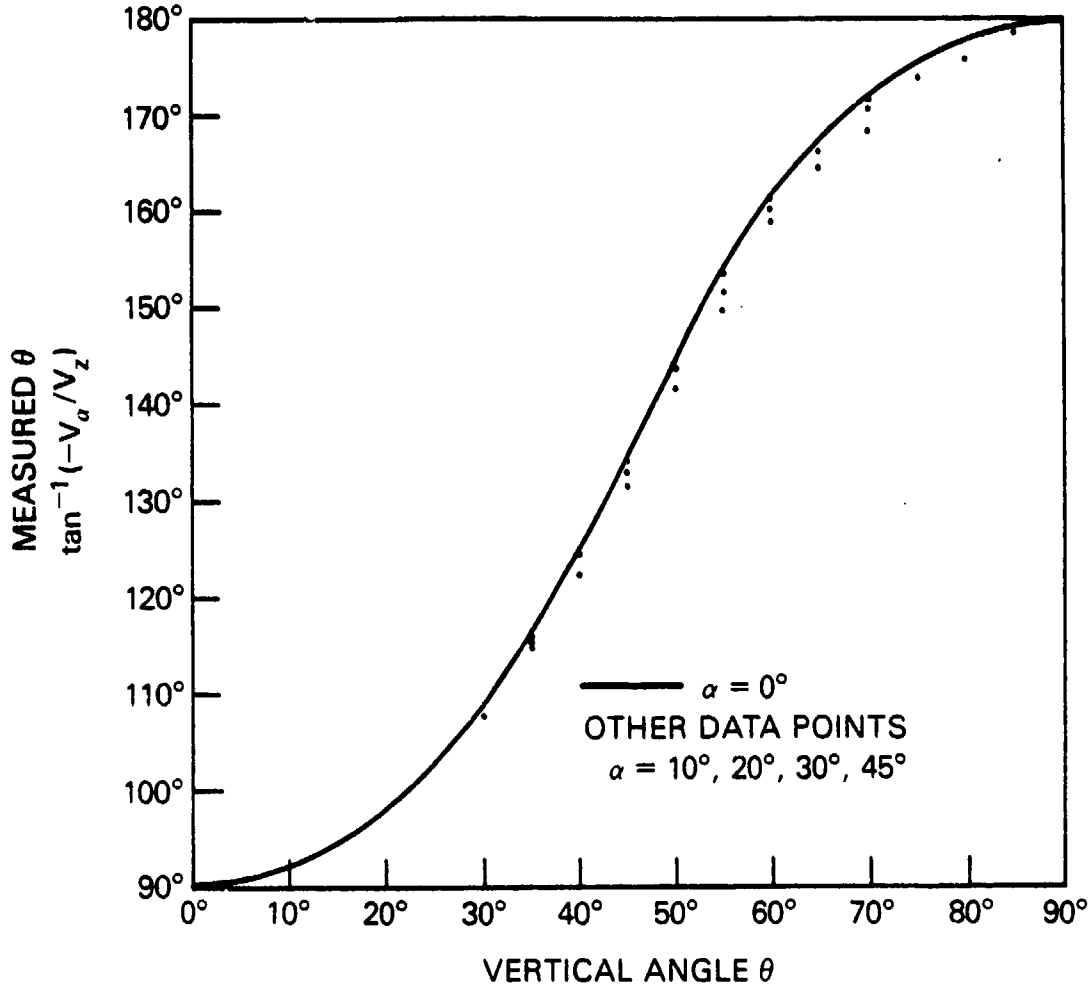


**Fig. 8 — Bearing measure for $k_a = 11$**

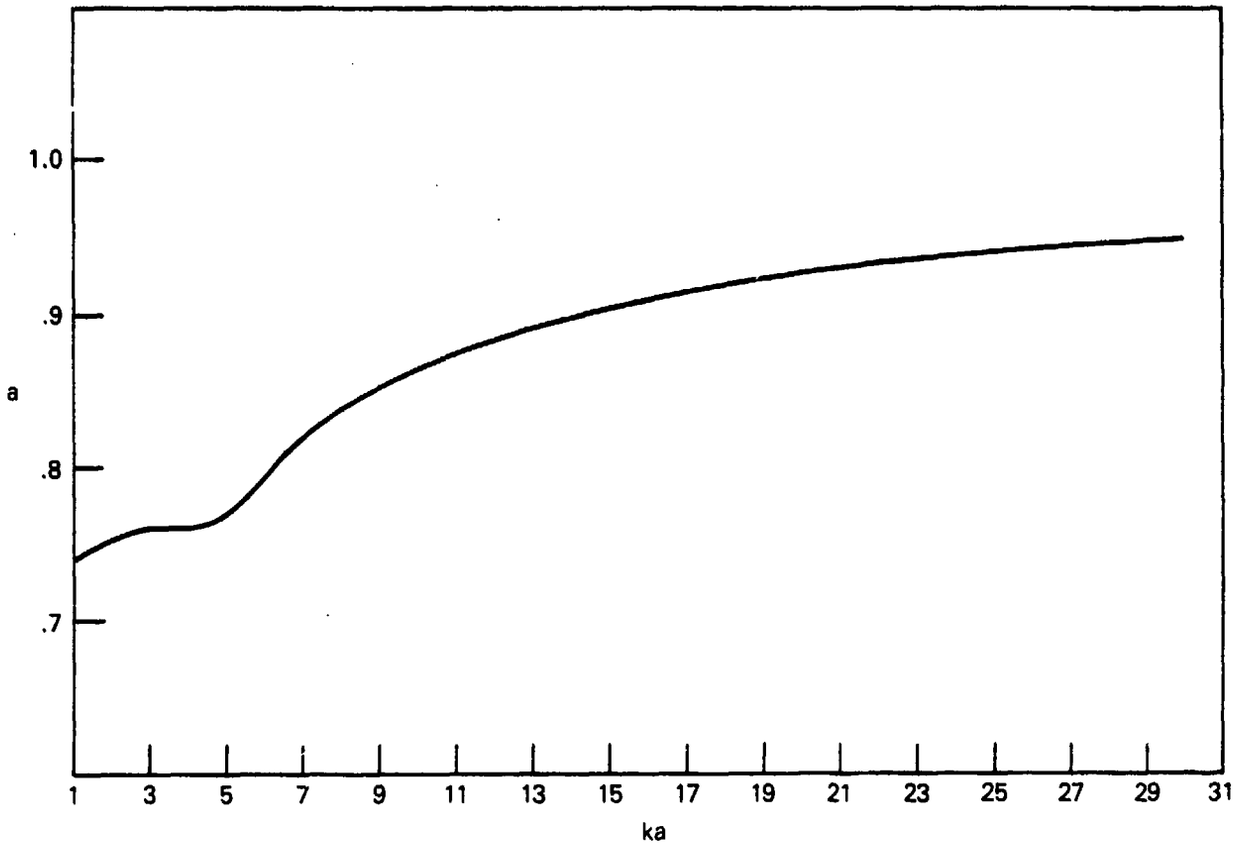


**Fig. 9 — Acoustic center of shaded hemisphere array**

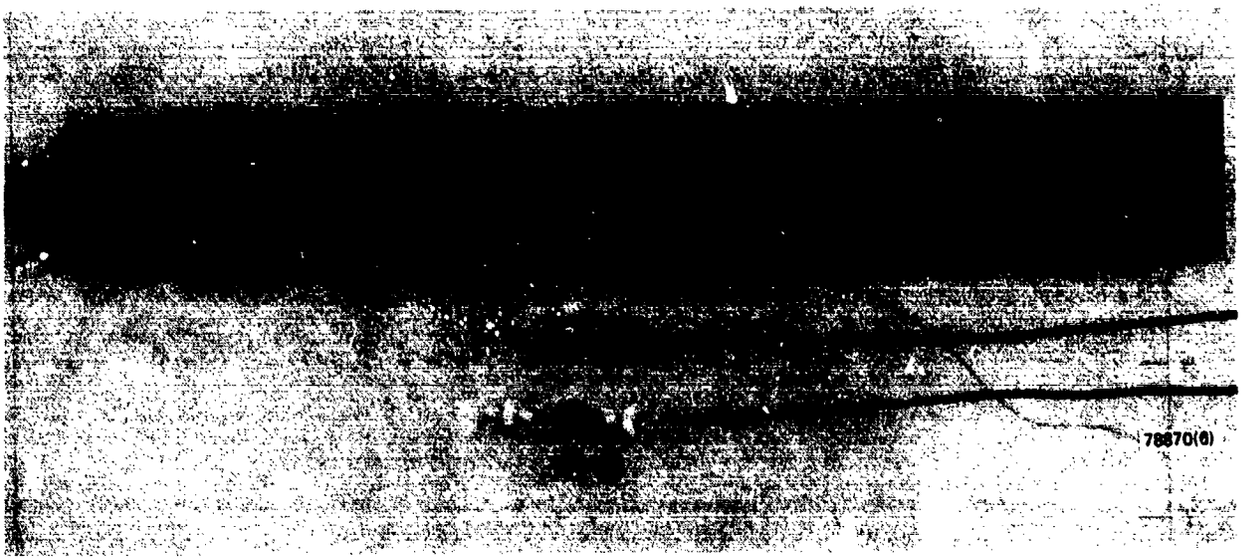


Fig. 10 — Experimental acoustic element components

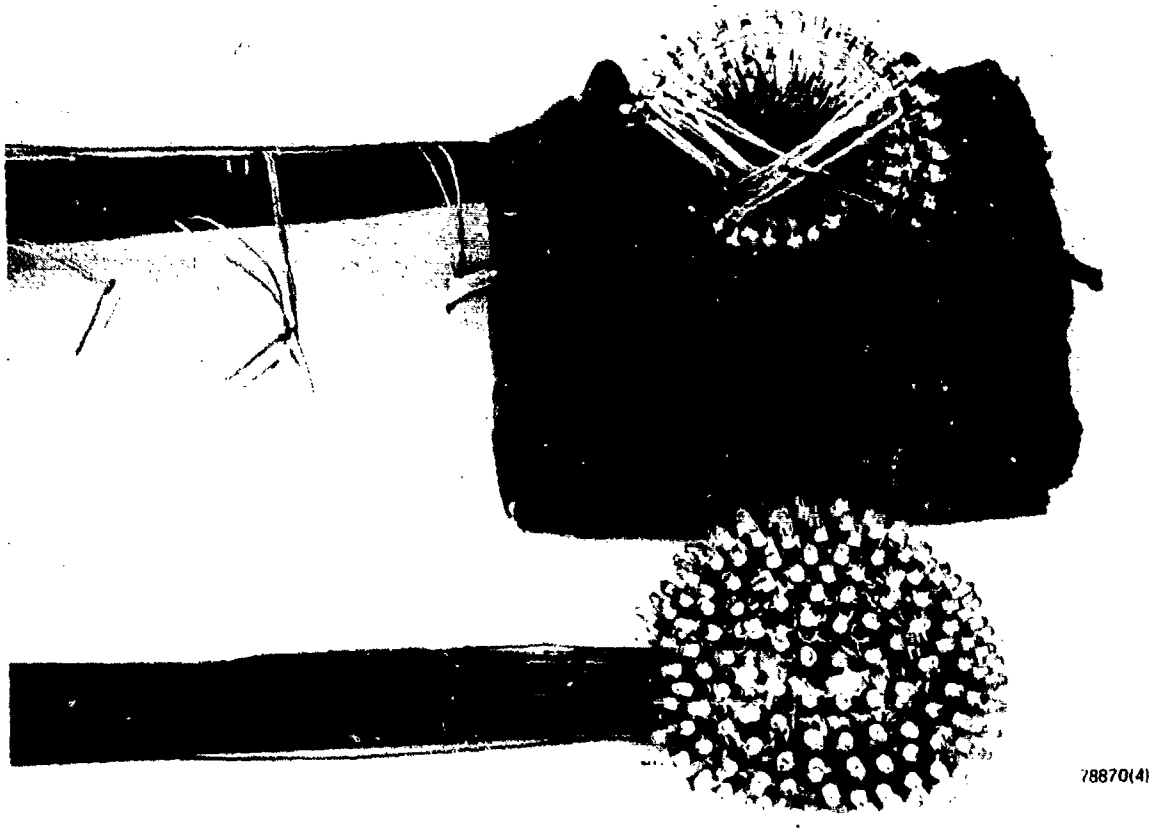

78870(4)

Fig. 11 — Assembled hemispheric array


Fig. 12 — Terminal board with shading capacitors

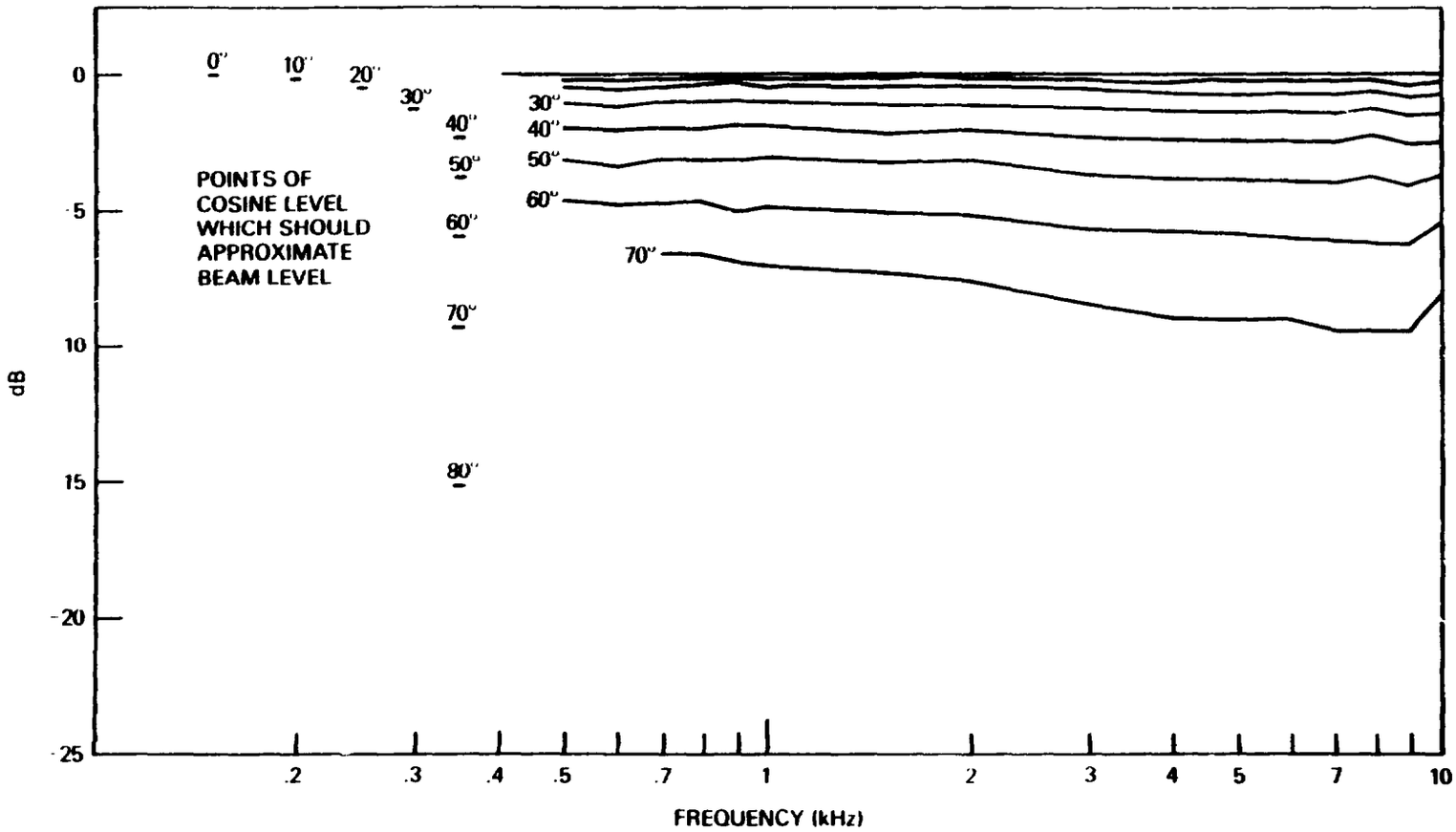


**Fig. 13 — Beam pattern for hemispheres in series, balanced output**

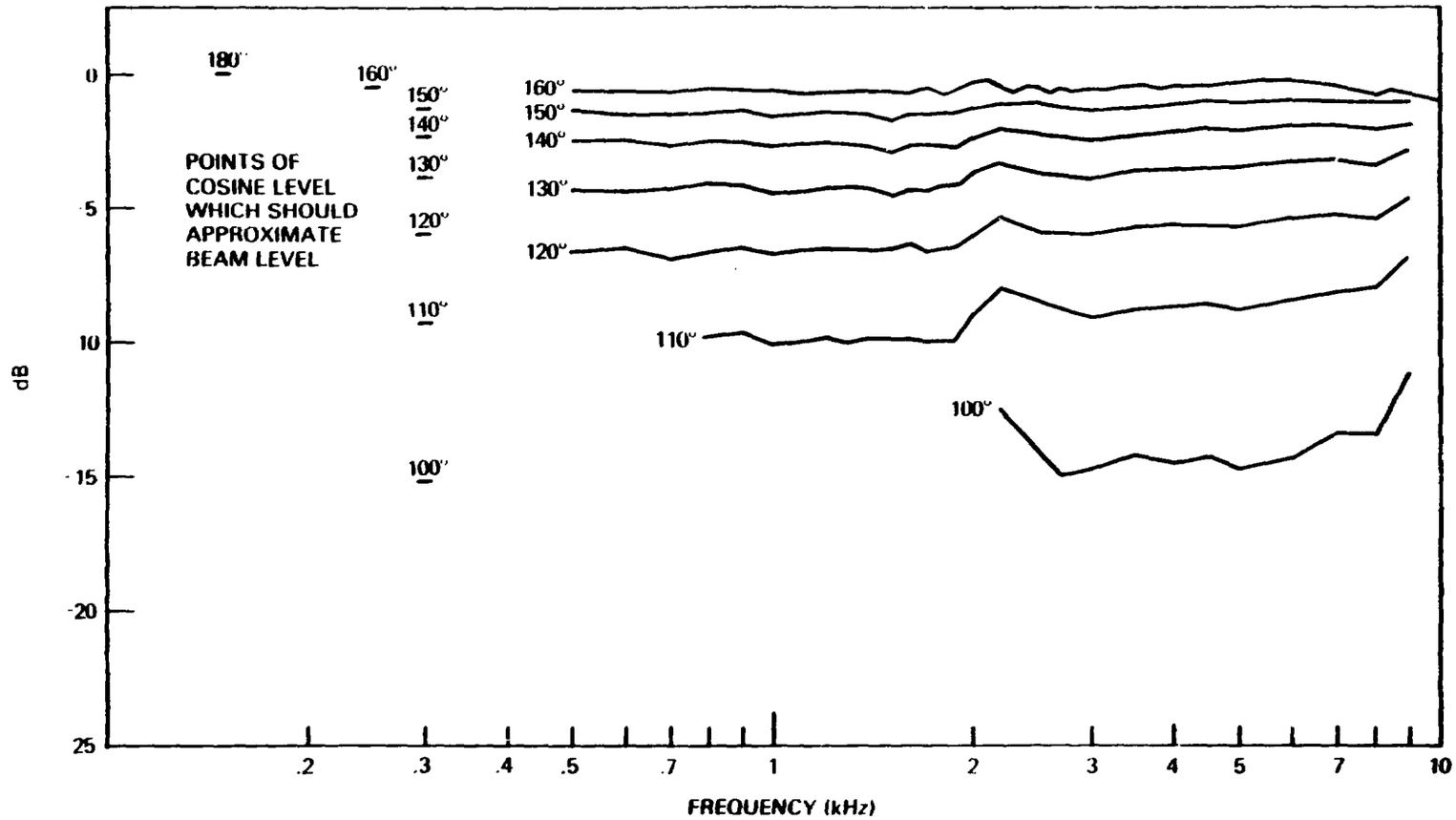


**Fig. 14 — Constant directivity (continuation of Fig. 13)**

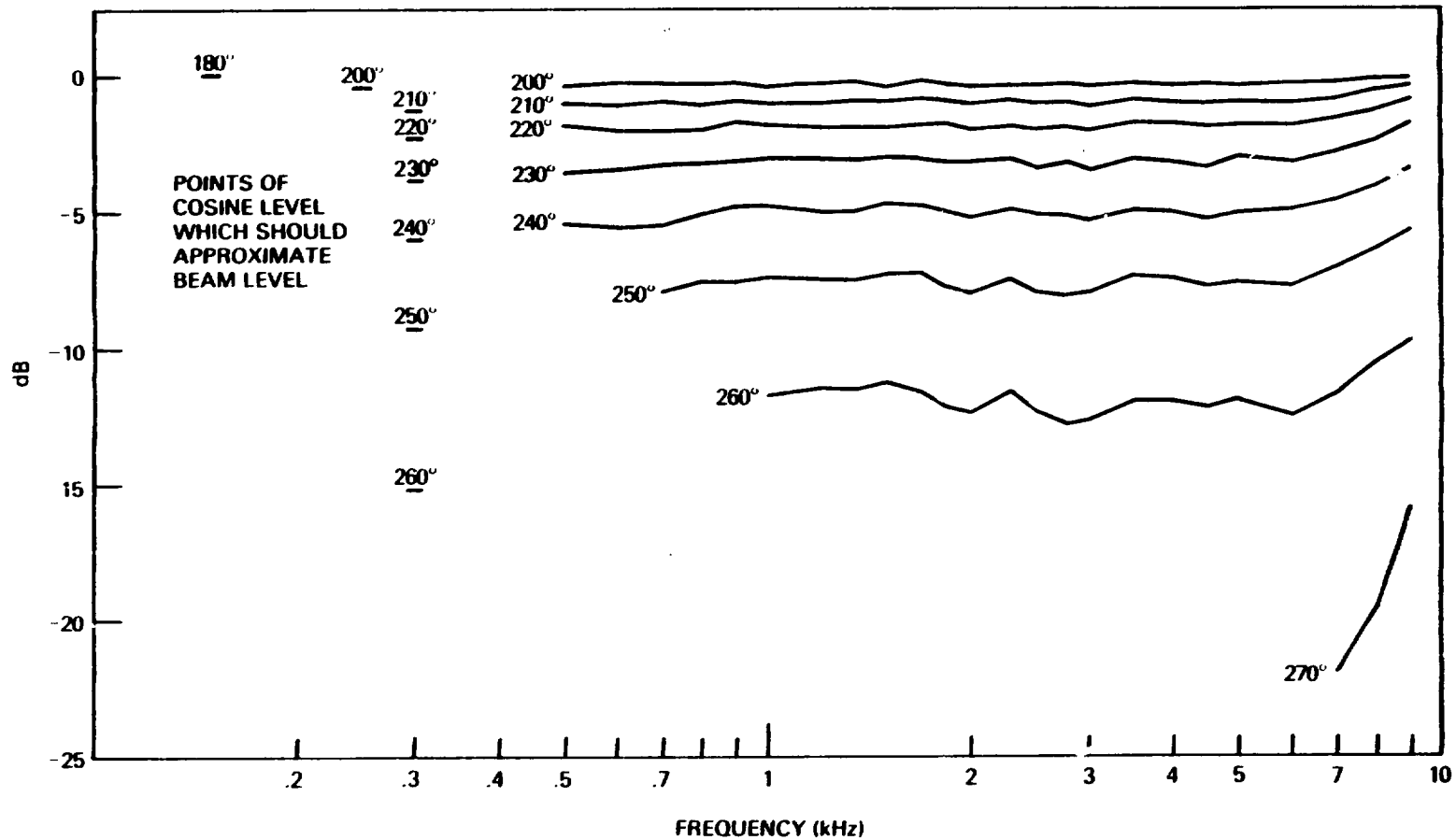


**Fig. 15 — Constant directivity (continuation of Fig. 14)**

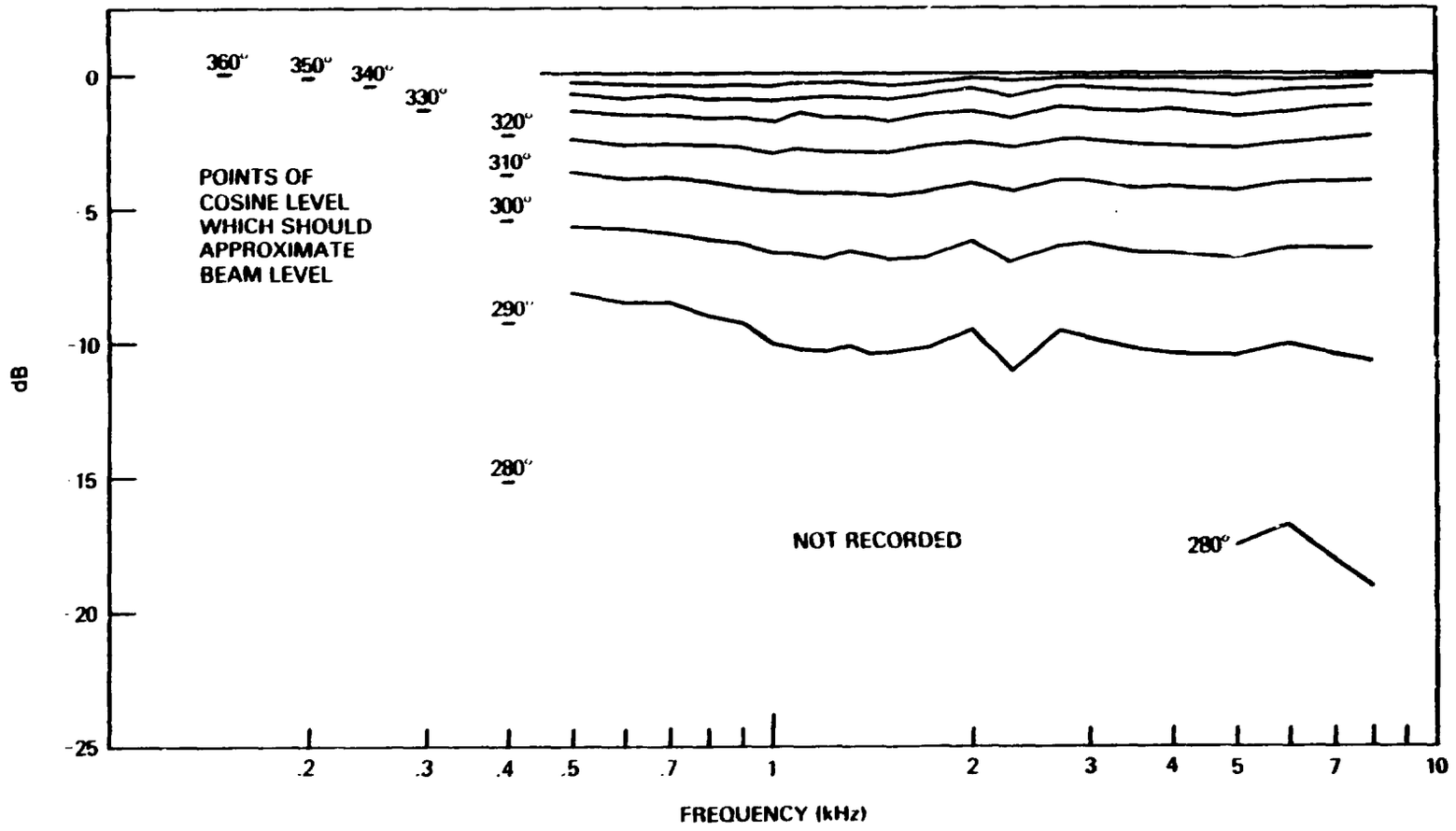


**Fig. 16 — Constant directivity (continuation of Fig. 15)**

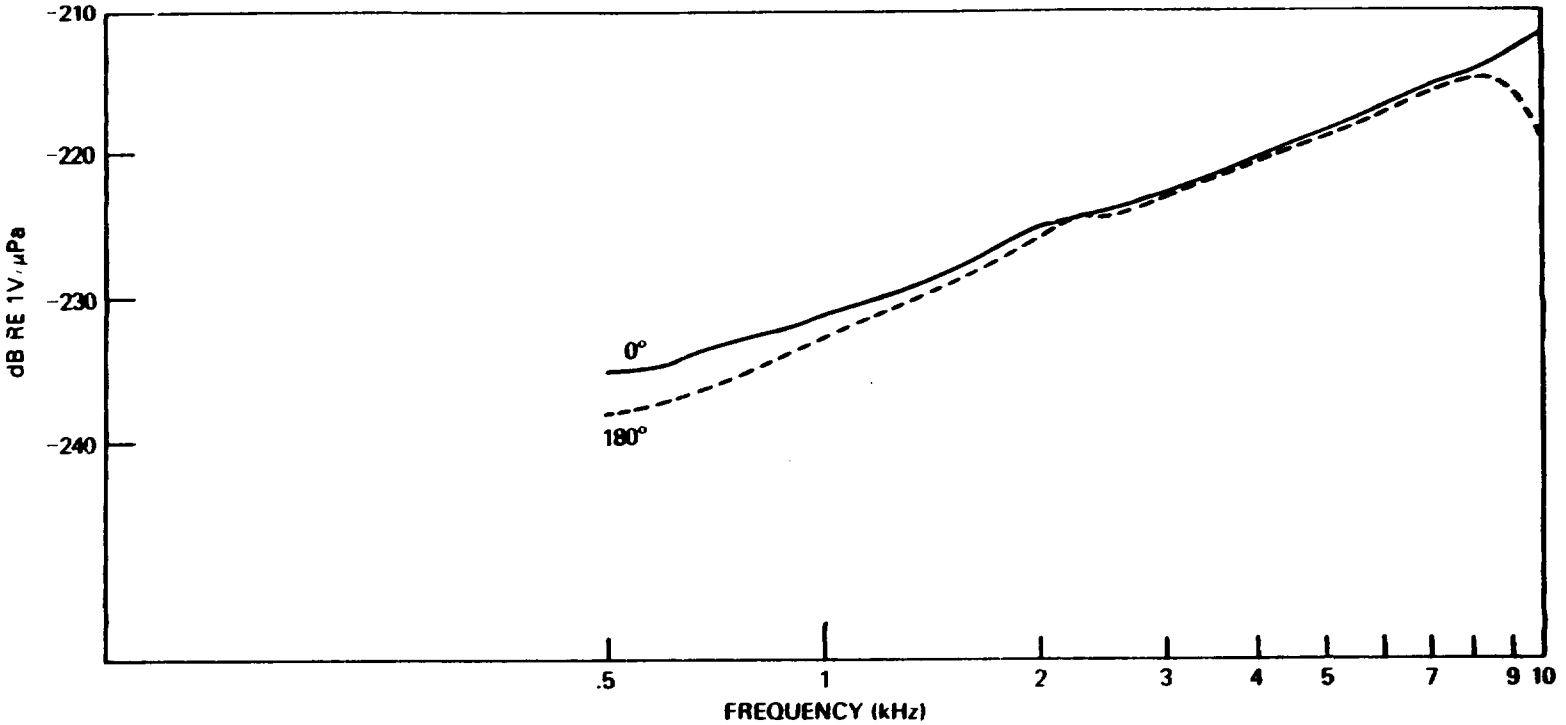


**Fig. 17 — Free-field voltage sensitivity for balanced output**

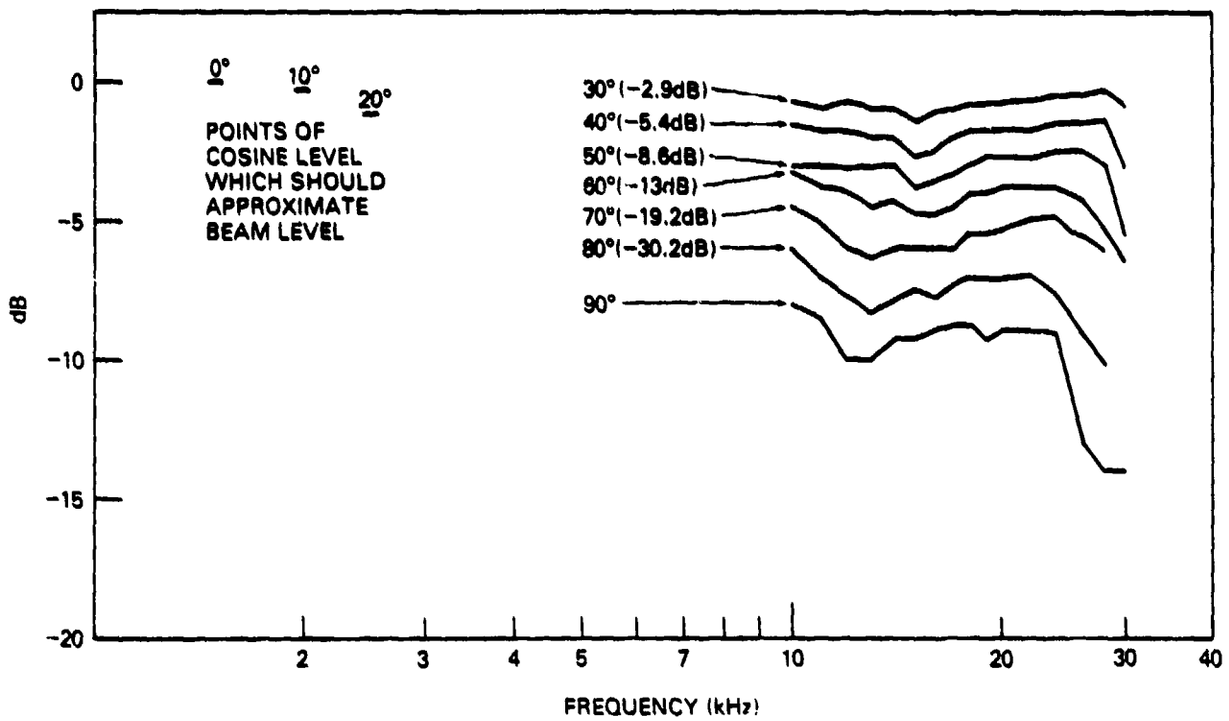


Fig. 18 — Hemisphere directivity for 0° hemisphere, unbalanced output

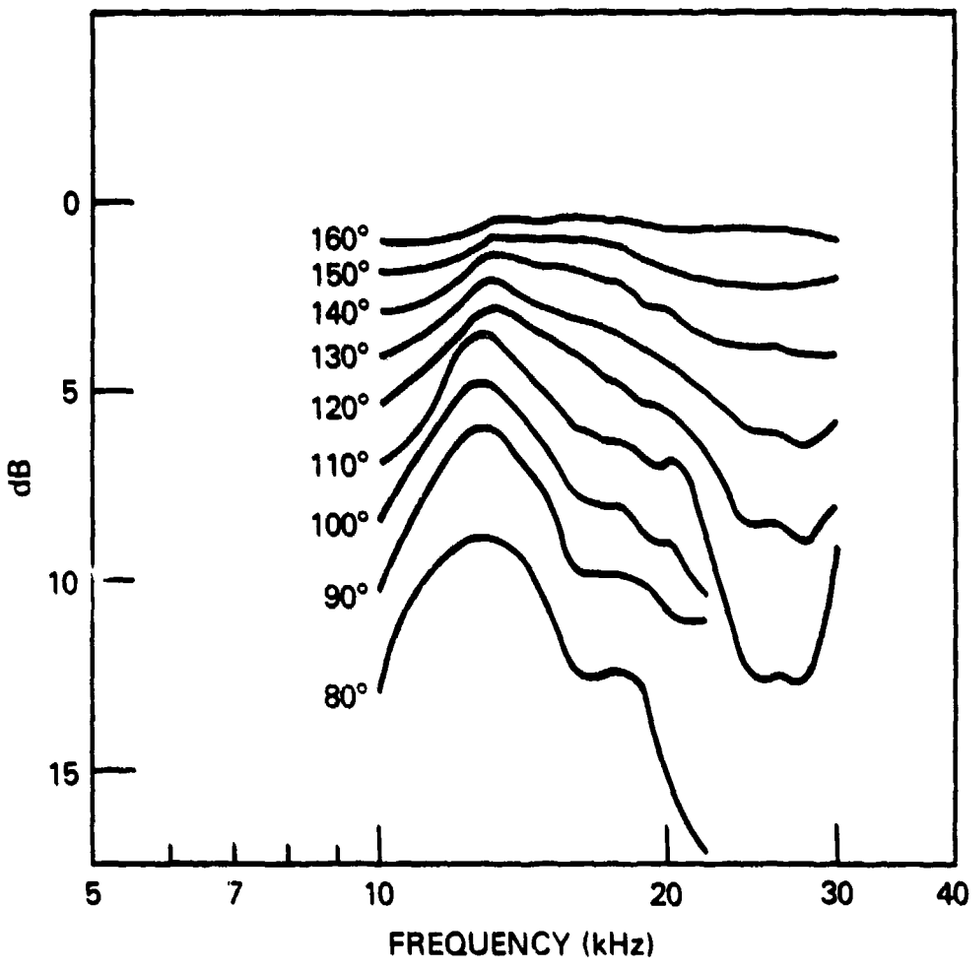


Fig. 19 — Hemisphere directivity for 180° hemisphere, unbalanced output

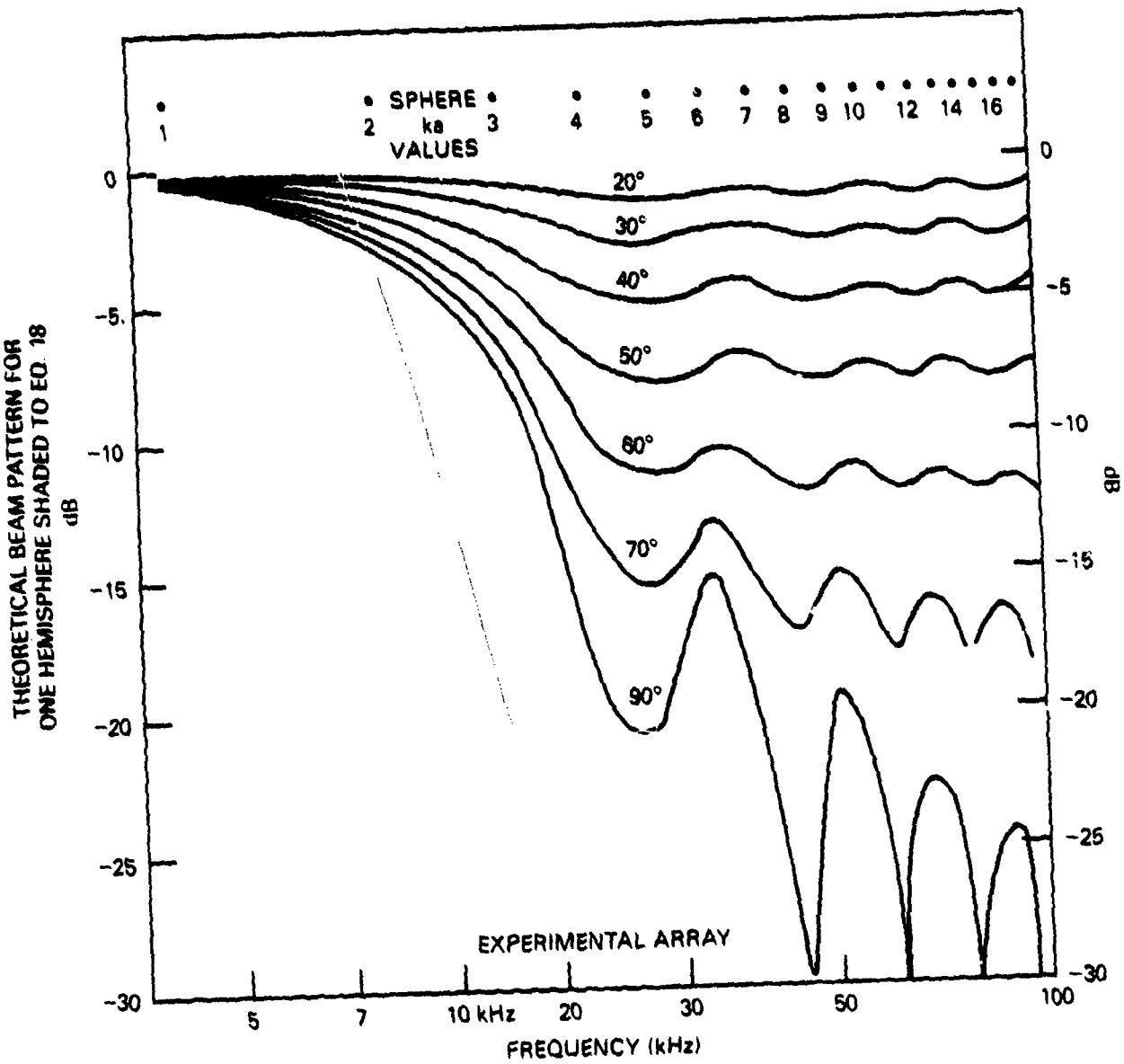


**Fig. 20 — Calculated directivity (5-100 kHz)**

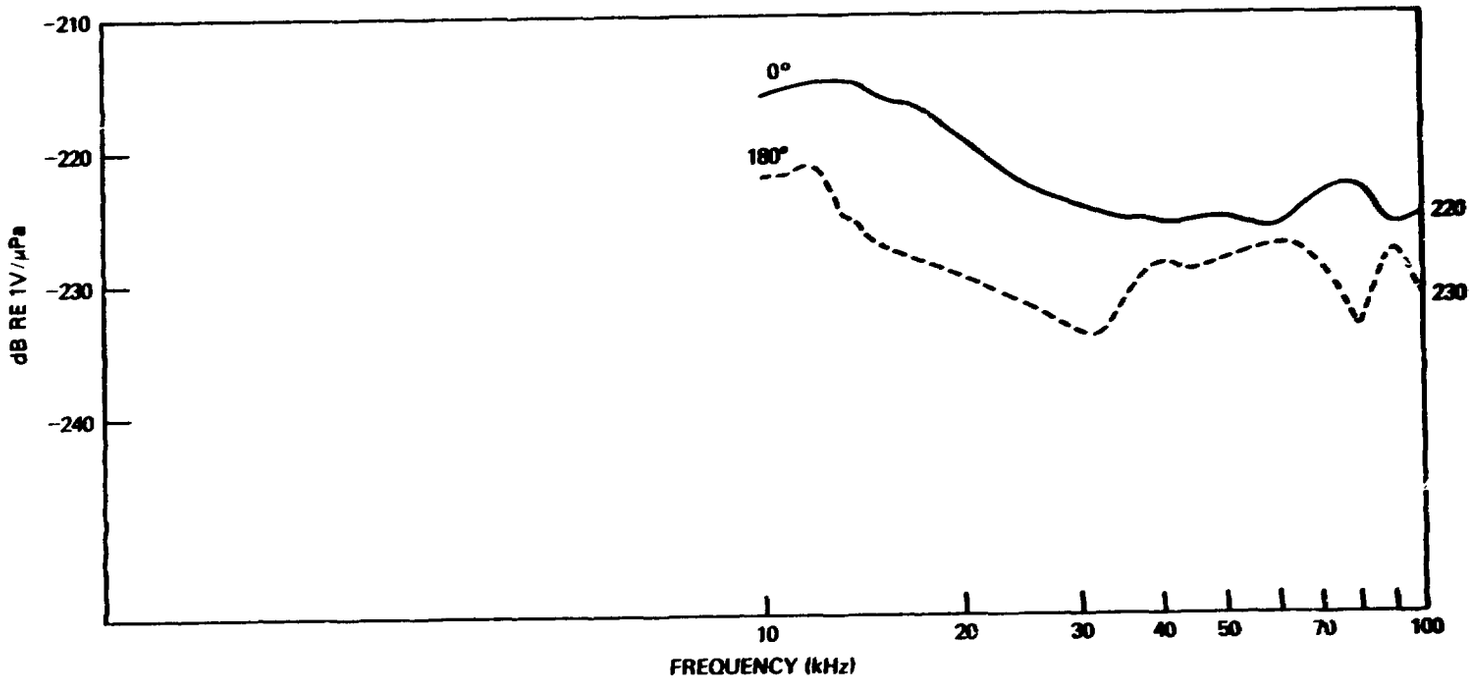


**Fig. 21 — Free-field voltage sensitivity (0° hemisphere)**

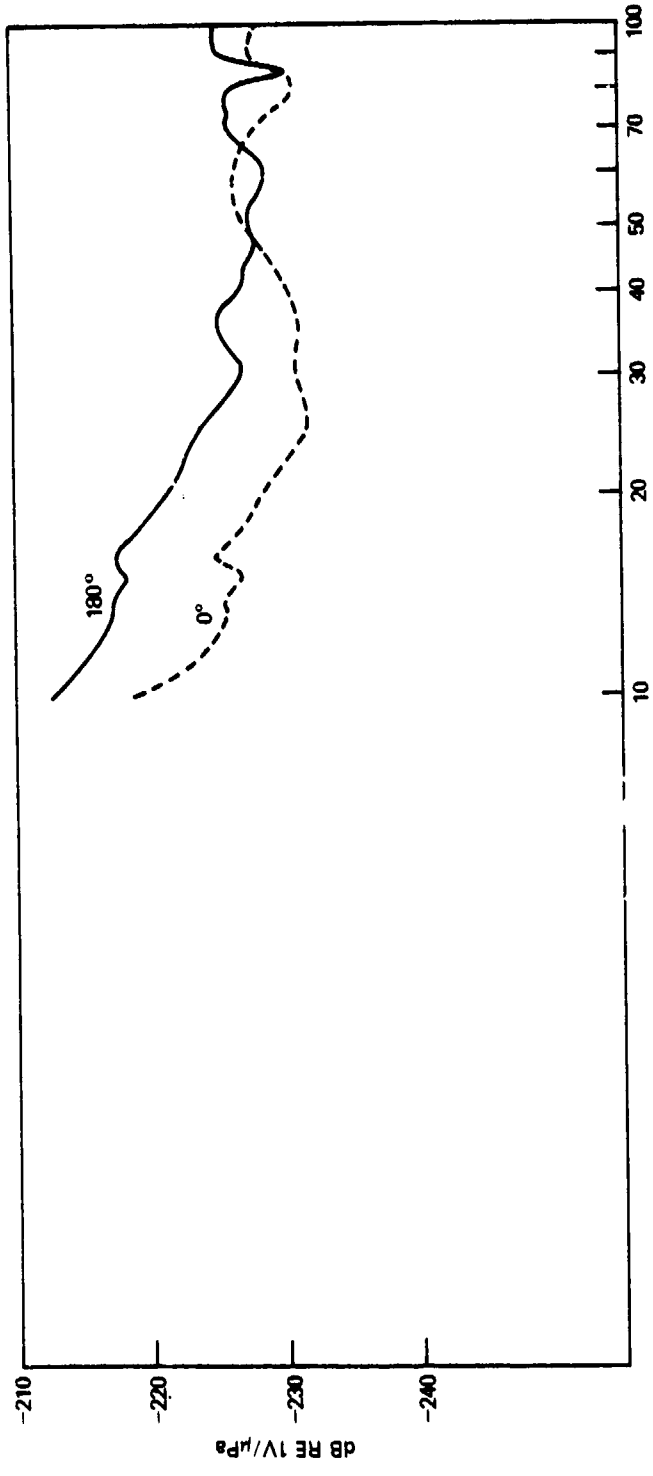


Fig. 22 — Free-field voltage sensitivity (180° hemisphere)

## 8.0 REFERENCES


1. R.A. Langevin, "The Electro-acoustic Sensitivity of Cylindrical Ceramic Tubes," Journal of Acoustical Society of America 26, 421 (1954) and 34, 1139 (1962).

2. W. J. Trott, "Sensitivity of Piezoceramic Tubes, With Capped or Shielded Ends, Above the Omnidirectional Frequency Range," Journal of Acoustical Society of America 62, 565 (1977)

3. P. H. Rogers and J. F. Zalesak, "Coefficients for Calculating Radiation Impedances and Far-field Pressures of Free-flooded Ring Transducers," Naval Research Laboratory Report 7749 (1974)

4. P. H. Rogers, ""SHIP" (Simplified Helmholtz-Integral Program), A Fast Computer Program for Calculating the Acoustic Radiation and Radiation Impedance for Free-flooded Ring and Finite-Circular-Cylinder Sources," Naval Research Laboratory Report 7240 (1972)

5. J. F. Zalesak and P. H. Rogers, "Low-Frequency Radiation Characteristics of Free-flooded Ring Transducers with Application to a Low-Frequency Directional Hydrophone," Journal of Acoustical Society of America 56, 1052 (1974)

6. W. J. Trott, "Design Theory for a Constant-Beamwidth Transducer", Naval Research Laboratory Report 7933 (1975)

7. P. H. Rogers and A. L. VanBuren, "New Approach to a Constant Beamwidth Transducer," Journal of Acoustical Society of America 64, 38 (1978)

8. J. Jarzynski and W. J. Trott, Array Shading for a Broadband Constant Directivity Transducer. Journal of Acoustical Society of America 64, 1266 (1978).

9. J. A. Bucaro, H. D. Dardy and E. F. Carome, "Fiber Optic Hydrophone", Appl. Opt. 16, 1761 (1977).